Synchronization in von Bertalanffy's models

J. Leonel Rocha[1], Sandra M. Aleixo[1] and Acilina Caneco[2]

[1] Instituto Superior de Engenharia de Lisboa - ISEL, ADM and CEAUL, Rua Conselheiro Emídio Navarro, 1, 1959-007 Lisboa, Portugal
   (E-mail: `jrocha@adm.isel.pt, sandra.aleixo@adm.isel.pt`),
[2] Instituto Superior de Engenharia de Lisboa - ISEL, ADM and CIMA-UE, Rua Conselheiro Emídio Navarro, 1, 1959-007 Lisboa, Portugal
   (E-mail: `acilina@adm.isel.pt`)

Abstract. Many data have been useful to describe the growth of marine mammals, invertebrates and reptiles, seabirds, sea turtles and fishes, using the logistic, the Gompertz and von Bertalanffy's growth models. A generalized family of von Bertalanffy's maps, which is proportional to the right hand side of von Bertalanffy's growth equation, is studied and its dynamical approach is proposed. The system complexity is measured using Lyapunov exponents, which depend on two biological parameters: von Bertalanffy's growth rate constant and the asymptotic weight.

Applications of synchronization in real world is of current interest. The behavior of birds flocks, schools of fish and other animals is an important phenomenon characterized by synchronized motion of individuals. In this work, we consider networks having in each node a von Bertalanffy's model and we study the synchronization interval of these networks, as a function of those two biological parameters. Numerical simulation are also presented to support our approaches.

Keywords: Von Bertalanffy's models, synchronization, Lyapunov exponents.

1 Introduction and motivation

Several mathematical equations have been used to describe the growth of marine populations, namely fishes, seabirds, marine mammals, invertebrates, reptiles and sea turtles. Among these equations, three of the most familiar are the logistics, the Gompertz and the von Bertalanffy models, see [8] and references therein. For a certain population, the growth of an individual, regarded as an increase in its length or weight with increasing age, is commonly modeled by a mathematical equation that represents the growth of an "average" individual in the population. One of the most popular functions that have been used to analyze the increase in average length or weight of fish is von Bertalanffy's model, see for example [2] and [5].

Synchronization is a fundamental nonlinear phenomenon, which can be observed in many real systems, in physics, chemistry, mechanics, engineering, secure communications or biology, see for example [1]. It can be observed in

living beings, on the level of single cells, physiological subsystems, organisms and even on the level of large populations. Sometimes, this phenomenon is essential for a normal functioning of a system, e.g. for the performance of a pacemaker, where the synchronization of many cells produce a macroscopic rhythm that governs respiration and heart contraction. Sometimes, the synchrony leads to a severe pathology, e.g. in case of the Parkinson's disease, when locking of many neurons leads to the tremor activity. Biological systems use internal circadian clocks to efficiently organize physiological and behavioral activity within the 24-hour time domain. For some species, social cues can serve to synchronize biological rhythms. Social influences on circadian timing might function to tightly organize the social group, thereby decreasing the chances of predation and increasing the likelihood of mating, see [4]. Almost all seabirds breed in colonies; colonial and synchronized breeding is hypothesized to reduce predation risk and increases social interactions, thereby reducing the costs of breeding . On the other hand, it is believed that synchronization may promote extinctions of some species. Full synchronism may have a deleterious effect on population survival because it may lead to the impossibility of a recolonization in case of a large global disturbance, see [16]. Understand the aggregate motions in the natural world, such as bird flocks, fish schools, animal herds, or bee swarms, for instance, would greatly help in achieving desired collective behaviors of artificial multi-agent systems, such as vehicles with distributed cooperative control rules.

The layout of this paper is as follows. In Sec.2, we present a new dynamical approach to von Bertalanffy's growth equation, a family of unimodal maps, designated by von Bertalanffy's maps. In Sec.3, we present the network model having in each node a von Bertalanffy's model. The synchronization interval is presented in terms of the network connection topology, expressed by its Laplacian matrix and of the Lyapunov exponent of the network's nodes. In Sec.4, we give numerical simulations on some kinds of lattices, evaluating its synchronization interval. We present some discussion on how this interval changes with the increasing of the number of neighbors of each node, with the increasing of the total number of nodes and with the intrinsic growth rate. We also observe and discuss some desynchronization phenomenon.

2   Von Bertalanffy's growth dynamics approach

An usual form of von Bertalanffy's growth function, one of the most frequently used to describe chick growth in marine birds and in general marine growths, is given by

$$W_t = W_\infty \left(1 - e^{-\frac{K}{3}(t-t_0)}\right)^3, \tag{1}$$

where W_t is the weight at age t, W_∞ is the asymptotic weight, K is von Bertalanffy's growth rate constant and t_0 is the theoretical age the chick would have at weight zero. The growth function, Eq.(1), is solution of the von Bertalanffy's
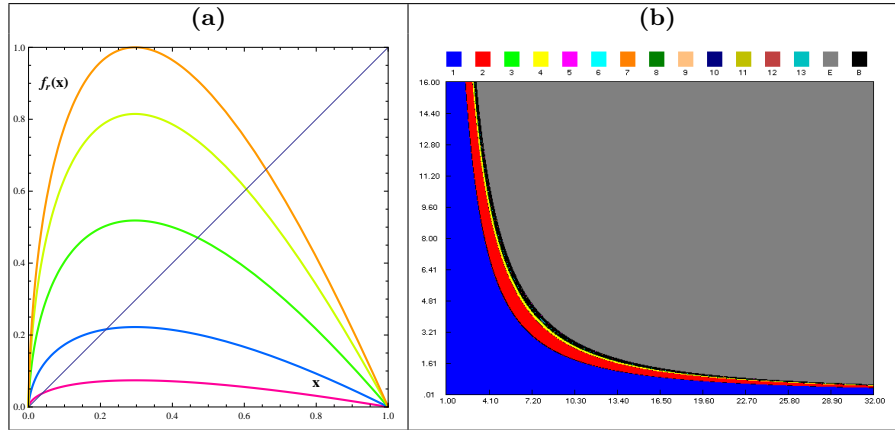
Fig. 1. (a) Graphics of von Bertalanffy's maps $f_r(x)$, Eq.(4), for several values of intrinsic growth rate r (0.5 (magenta), 1.5, 3.5, 5.5 and 6.75 (orange)); (b) Bifurcation diagram of von Bertalanffy's maps $f_r(x)$ in the (K, W_∞) parameter plane. The blue region is the stability region. The period doubling and chaotic regions correspond to the cycles shown on top of figure. The gray region is the non admissible region.

growth equation,

$$g(W_t) = \frac{dW_t}{dt} = \frac{K}{3} \, W_t^{\frac{2}{3}} \left(1 - \left(\frac{W_t}{W_\infty} \right)^{\frac{1}{3}} \right), \tag{2}$$

introduced by von Bertalanffy to model fish weight growth, see [17] and [18]. The *per capita* growth rate, associated to this growth model, is given by

$$h(W_t) = \frac{g(W_t)}{W_t} = \frac{K}{3} \, W_t^{-\frac{1}{3}} \left(1 - \left(\frac{W_t}{W_\infty} \right)^{\frac{1}{3}} \right). \tag{3}$$

In this paper, we consider a family of unimodal maps, the von Bertalanffy maps, which is proportional to the right hand side of von Bertalanffy's equation, Eq.(2), $f_r : [0, 1] \to [0, 1]$, defined by

$$f_r(x) = r \, x^{\frac{2}{3}} \left(1 - x^{\frac{1}{3}} \right), \tag{4}$$

with $x = \frac{W_t}{W_\infty} \in [0, 1]$ the normalized weight and $r = r(K, W_\infty) = \frac{K}{3} \times W_\infty^{\frac{2}{3}} > 0$ an intrinsic growth rate of the individual weight, see Fig.1(a).

Remark that, the family of maps that we will study depends on two biological parameters: von Bertalanffy's growth rate constant K and the asymptotic weight W_∞. The following conditions are satisfied:

(A1) f_r is continuous on $[0, 1]$;

(A2) f_r has an unique critical point $c = (2/3)^3 \in]0, 1[$;

(A3) $f_r'(x) \neq 0, \forall x \in]0, 1[\backslash \{c\}$, $f_r'(c) = 0$ and $f_r''(c) < 0$;

(A4) $f_r \in C^3\left(\left]0,1\right[\right)$ and the Schwarzian derivative of f_r, denoted by $S\left(f_r(x)\right)$, verifies $S\left(f_r(x)\right) < 0, \forall x \in \left]0,1\right[\setminus\{c\}$ and $S\left(f_r(c)\right) = -\infty$.

Conditions $(A1)-(A4)$ are essential to prove the stability of the only positive fixed point, [15]. In particular, the negative Schwarzian derivative ensures a "good" dynamic behavior of the models. In general, the growth models studied have negative Schwarzian derivative and the use of unimodal maps is usual, see for example [12] and [13].

The dynamical complexity of the proposed models is displayed at (K, W_∞) parameter plane, depending on the variation of the intrinsic growth rate r. The analysis of their bifurcations structure is done based on the bifurcation diagram, see Fig.1(b). For these models, the extinction region and the semistability curve have no expressive meaning. Because it is difficult to identify *per capita* growth rates, Eq.(3), less than one for all densities, to the extinction case, and *per capita* growth rates strictly less than one for all densities, except at one population density, to the semistability case, except at most a set of measure zero. We verify that, $\lim\limits_{x \to 0^+} f_r'(x) > 1$ and the origin's basin of attraction is empty, except at most a set of measure zero. The fixed point 0 is unstable.

A behavior of stability is defined when a population persists for intermediate initial densities and otherwise goes extinct. The *per capita* growth rate of the population, Eq.(3), is greater than one for an interval of population densities. The lower bound of these densities correspond to the positive fixed point

$$A_{K,W_\infty} \equiv A_r = \left(\frac{r}{r+1}\right)^3,$$

of each function f_r, Eq.(4), see Fig.1(a). Furthermore, attending to $(A2)$ and $(A3)$ we have that $f_r^2\left(c\right) > 0$, then there is a linearly stable fixed point $A_r \in \left]0,1\right[$, whose basin of attraction is $\left]0,1\right[$. For more details see [15].

The symbolic dynamics techniques prove to be a good method to determine a numerical approximation to the stability region (in blue), see Fig.1(b). For more details about symbolic dynamics techniques see for example [12]. In the (K, W_∞) parameter plane, this region is characterized by the critical point iterates that are always attracted to the fixed point sufficiently near of the super stable or super attractive point $\tilde{A}_r$, defined by $f_r\left(c\right) = c$. Let $\bar{A}_r \in \left]0,1\right[$ be the fixed points sufficiently near of $\tilde{A}_r$, then

$$\lim\limits_{n \to \infty} f_r^n\left(c\right) = \bar{A}_r, \quad \text{for} \quad \left(3K^{-1}A_r^{\frac{1}{3}}\left(1 - A_r^{\frac{1}{3}}\right)\right)^{\frac{3}{2}} < W_\infty(K) < \hat{W}_\infty(K)$$

where $\hat{W}_\infty(K)$ represents the super stable curve of the cycle of order 2, given in implicit form by $f_r^2\left(c\right) = c$. In this parameter plane, the set of the super stable or super attractive points $\tilde{A}_r$ defines the super stable curve of the fixed point. In the region before reaching the super stable curve, the symbolic sequences associated to the critical points orbits are of the type CL^∞. After this super stable curve, the symbolic sequences are of the type CR^∞. In this parameter region, the topological entropy is null, [10].

The period doubling region corresponds to the parameters values, to which the population weight oscillates asymptotically between 2^n states, with $n \in \mathbb{N}$.

In period-doubling cascade, the symbolic sequences correspondent to the iterates of the critical points are determined by the iterations $f_r^{2^n}(c) = c$. Analytically, these equations define the super-stability curves of the cycle of order 2^n. The period doubling region is bounded below by the curve of the intrinsic growth rate values where the period doubling starts, $\hat{W}_\infty(K)$, correspondent to the 2-period symbolic sequences $(CR)^\infty$. Usually, the upper bound of this region is determined using values of intrinsic growth rate r, corresponding to the first symbolic sequence with non null topological entropy. Commonly, the symbolic sequence that identifies the beginning of chaos is $\left(CRLR^3\right)^\infty$, a 6-periodic orbit, see for example [12] and [13]. The unimodal maps in this region, also have null topological entropy, [10].

In the chaotic region of the (K, W_∞) parameter plane, the evolution of the population size is *a priori* unpredictable. The maps are continuous on the interval with positive topological entropy whence they are chaotic and the Sharkovsky ordering is verified. The symbolic dynamics are characterized by iterates of the functions f_r that originate orbits of several types, which already present chaotic patterns of behavior. The topological entropy is a non-decreasing function in order to the parameter r, until reaches the maximum value ln 2 (consequence of the negative Schwartzian derivative). In [12] and [13] can be seen a topological order with several symbolic sequences and their topological entropies, which confirm this result to others growth models. This region is bounded below by the curve of the intrinsic growth rate values where the chaos starts. The upper bound is the *fullshift* curve or chaotic semistability curve, defined by $f_r(c) = 1$. This curve characterizes the transition between the chaotic region and the non admissible region. In the non admissible region, the graphic of any function f_r is no longer totally in the invariant set $[0, 1]$. The maps under these conditions no longer belong to the studied family functions and are not good models for populations dynamics.

The above explanations are summarized in the next result:

Lemma 1. *Let $f_r(x)$ be von Bertalanffy's maps, Eq.(4), with $r \in \mathbb{R}^+$ and satisfying $(A1) - (A4)$.*

(i) *(Stability region of the fixed point A_r) If $0 < r < 5$, then there is a linearly stable fixed point $A_r \in \,]0, 1[$ whose basin of attraction is $]0, 1[$;*

(ii) *(Period doubling and chaotic regions) If $5 < r < \frac{3^3}{2^2}$, then the interval $[f_r^2(c), f_r(c)]$ is forward invariant with basin of attraction $]0, 1[$;*

(iii) *(Chaotic semistability curve) If $r = \frac{3^3}{2^2}$, then $[0, 1]$ is invariant and verifies that*

$$\bigcup_{n \geq 0} f_r^n(x) = [0, 1] \quad and \quad \lim_{n \to \infty} \frac{1}{n} |Df_r^n(x)| > 0,$$

for Lebesgue almost every $x \in [0, 1]$.

For more analytical details of the proof see [14] and [15].

3   Synchronization and Lyapunov exponents

Consider a general network of N identical coupled dynamical systems, described by a connected, undirected graph, with no loops and no multiple edges. In each node the dynamics of the system is defined by the maps f_r given by Eq.(4). The state equations of this network, in the discretized form, are

$$x_i(k+1) = f_r(x_i(k)) + c \sum_{j=1}^{N} l_{ij} x_j(k), \text{ with } i = 1, 2, ..., N \qquad (5)$$

where c is the coupling parameter and $L = (l_{ij})$ is the Laplacian matrix or coupling configuration of the network. The Laplacian matrix is given by $L = D - A$, where A is the adjacency matrix and $D = (d_{ij})$ is a diagonal matrix, with $d_{ii} = k_i$, being k_i the degree of node i. The eigenvalues of L are all real and non negatives and are contained in the interval $[0, \min\{N, 2\Delta\}]$, where Δ is the maximum degree of the vertices. The spectrum of L may be ordered, $\lambda_1 = 0 \leq \lambda_2 \leq \cdots \leq \lambda_N$. The network (5) achieves asymptotical synchronization if

$$x_1(t) = x_2(t) = ... = x_N(t) \underset{t \to \infty}{\to} e(t),$$

where $e(t)$ is a solution of an isolated node (equilibrium point, periodic orbit or chaotic attractor), satisfying $\dot{e}(t) = f(e(t))$.

One of the most important properties of a chaotic system is the sensitivity to initial conditions. A way to measure the sensitivity with respect to initial conditions is to compute the average rate at which nearby trajectories diverge from each other. Consider the trajectories x_k and y_k, starting, respectively, at x_0 and y_0. If both trajectories are, until time k, always in the same linear region, we can write

$$|x_k - x_k| = e^{\lambda k}|x_0 - y_0|, \text{ where } \lambda = \frac{1}{k} \sum_{j=0}^{k-1} \ln |f_r'(x_j)|.$$

The Lyapunov exponents of a trajectory x_k is defined by

$$h_{\max} = \lim_{k \to +\infty} \frac{1}{k} \sum_{j=0}^{k-1} \ln |f_r'(x_j)| \qquad (6)$$

whenever it exists. The computation of the Lyapunov exponent $h_{\max}$ gives the average rate of divergence (if $h_{\max} > 0$), or convergence (if $h_{\max} < 0$) of the two trajectories from each other, during the time interval $[0, k]$, see for example [6]. We note that, the Lyapunov exponents depend on two biological parameters: von Bertalanffy's growth rate constant and the asymptotic weight. See in Fig.2 the Lyapunov exponents estimate for von Bertalanffy's maps Eq.(4).

If the coupling parameter c belongs to the synchronization interval

$$\left] \frac{1 - e^{-h_{\max}}}{\lambda_2}, \frac{1 + e^{-h_{\max}}}{\lambda_N} \right[\qquad (7)$$

then the synchronized states $x_i(t)$, $(i = 1, ...N)$ are exponentially stable, [9]. The second eigenvalue λ_2 is know as the algebraic connectivity or Fiedler value
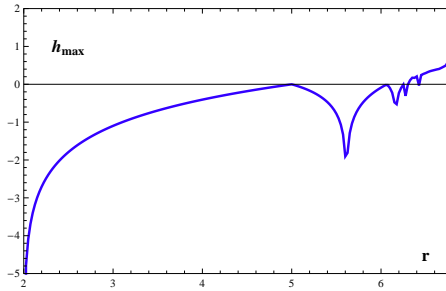
Fig. 2. Lypunov exponents estimates for von Bertalanffy's maps Eq.(4), as a function of the intrinsic growth rate r.

and plays a special role in the graph theory. As bigger is λ_2, more easily the network synchronizes. As much larger λ_2 is, more difficult is to separate the graph in disconnected parts. The graph is connected if and only if $\lambda_2 \neq 0$. In fact, the multiplicity of the null eigenvalue λ_1 is equal to the number of connected components of the graph. Fixing the topology of the network, the eigenvalues of the Laplacian λ_2 and λ_N are fixed, so the synchronization only depends on the Lyapunov exponent of each node, $h_{\max}$, which in turn depends on the two biological parameters: von Bertalanffy's growth rate constant and the asymptotic weight.

4 Numerical simulation and conclusions

To support our approaches, we consider a regular ring lattice, a graph with N nodes, each one connected to k neighbors, $\frac{k}{2}$ on each side, having in each node the same model, the von Bertalanffy maps f_r given by Eq.(4). See in Fig.3 some example of lattices. If, for instance, $N = 6$ and $K = 4$, see Fig.3c), the
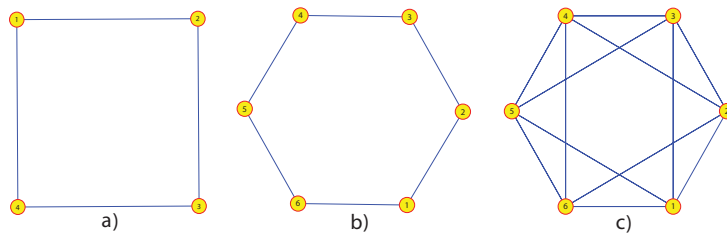

Fig. 3. Lattices. In a) with $N = 4$ nodes and $k = 2$, in b) with $N = 6$ nodes and $k = 2$ and in c) with $N = 6$ nodes and $k = 4$. From (a) to (b) the total number of vertices of the network increases maintaining the number of neighbors of each node, and from (b) to (c) increases the number of neighbors of each node, but the total number of vertices of the network remains the same.

adjacency matrix A and the Laplacian matrix L are

$$A = \begin{bmatrix} 0 & 1 & 1 & 0 & 1 & 1 \\ 1 & 0 & 1 & 1 & 0 & 1 \\ 1 & 1 & 0 & 1 & 1 & 0 \\ 0 & 1 & 1 & 0 & 1 & 1 \\ 1 & 0 & 1 & 1 & 0 & 1 \\ 1 & 1 & 0 & 1 & 1 & 0 \end{bmatrix} \quad \text{and} \quad L = D - A = \begin{bmatrix} 4 & -1 & -1 & 0 & -1 & -1 \\ -1 & 4 & -1 & -1 & 0 & -1 \\ -1 & -1 & 4 & -1 & -1 & 0 \\ 0 & -1 & -1 & 4 & -1 & -1 \\ -1 & 0 & -1 & -1 & 4 & -1 \\ -1 & -1 & 0 & -1 & -1 & 4 \end{bmatrix}.$$

So, the network correspondent to the graph in Fig.3 c) is defined by the system,

$$\begin{cases} \dot{x}_1 = f_r(x_1) + c(4x_1 - x_2 - x_3 - x_5 - x_6) \\ \dot{x}_2 = f_r(x_2) + c(-x_1 + 4x_2 - x_3 - x_4 - x_6) \\ \dot{x}_3 = f_r(x_3) + c(-x_1 - x_2 + 4x_3 - x_4 - x_5) \\ \dot{x}_4 = f_r(x_4) + c(-x_2 - x_3 + 4x_4 - x_5 - x_6) \\ \dot{x}_5 = f_r(x_5) + c(-x_1 - x_3 - x_4 + 4x_5 - x_6) \\ \dot{x}_6 = f_r(x_6) + c(-x_1 - x_2 - x_4 - x_5 + 4x_6) \end{cases}.$$

For this lattice the eigenvalues of the Laplacian matrix are $\lambda_1 = 0$, $\lambda_2 = \lambda_3 = \lambda_4 = 4$ and $\lambda_5 = \lambda_6 = 6$. If we consider, for instance, $r = 6.60$, the Lyapunov exponent of $f_r(x)$ is 0.377, Eq.(6). Then, attending to Eq.(7), this lattice synchronizes if $\frac{1-e^{-0.377}}{4} < c < \frac{1+e^{-0.377}}{6} \Leftrightarrow 0.079 < c < 0.281$ and the amplitude of the synchronization interval is 0.202. For more examples see Table 1. The lattice correspondent to the Fig.3 b) has eigenvalues of the Laplacian matrix $\lambda_1 = 0$, $\lambda_2 = \lambda_3 = 1$, $\lambda_4 = \lambda_5 = 3$ and $\lambda_6 = 4$. Thus, for the same $r = 6.60$, the lattice synchronizes if $0.313 < c < 0.421$ and the amplitude of this interval is 0.107. Moreover, to the lattice in Fig.3 a), the eigenvalues of the Laplacian matrix are $\lambda_1 = 0$, $\lambda_2 = \lambda_3 = 2$ and $\lambda_4 = 4$. For the same $r = 6.60$, the lattice synchronizes if $0.157 < c < 0.421$ and the amplitude of this interval is 0.264. In Table 1 are presented more examples, where we computed the synchronization interval for several values of the intrinsic growth rate r, for all these lattices a), b) and c) of Fig.3. The results of Table 1 allow us to claim:

(C1) From the lattice a) to lattice b) in Fig.3, the total number of vertices of the network increases maintaining the number of neighbors of each node. We verify that the synchronization is worse, not only because it begins to synchronize at a higher value of the coupling parameter c, but also, because the synchronization interval is shorter.

(C2) Comparing the results for the lattices b) and c) in Fig.3, we may conclude that maintaining the total number of vertices of the network, but increasing the number of neighbors of each node, the synchronization is better, not only because it begins to synchronize at a lower value of the coupling parameter c, but also, because the synchronization interval is larger.

(C3) Observing the columns of Table 1, we verify that, as the intrinsic growth rate r increases, the synchronization is worse, not just because it begins to synchronize at a higher value of the coupling parameter c, but also, because the synchronization interval is shorter.

(C4) Note that, for the intrinsic growth rate $r = 6.74$ and $r = 6.75$, for the lattice b), the upper bound of the synchronization interval is lower than the lower

r	h_{max}	Synchronization Interval			Amplitude		
		Lattice a)	Lattice b)	Lattice c)	Lattice a)	Lattice b)	Lattice c)
6.50	0.297	]0.128, 0.436[	]0.257, 0.436[	]0.064, 0.291[	0.308	0.179	0.226
6.55	0.347	]0.147, 0.427[	]0.293, 0.427[	]0.073, 0.285[	0.280	0.134	0.211
6.60	0.377	]0.157, 0.421[	]0.313, 0.421[	]0.079, 0.281[	0.264	0.107	0.202
6.65	0.406	]0.167, 0.417[	]0.334, 0.417[	]0.083, 0.278[	0.250	0.083	0.194
6.70	0.463	]0.185, 0.407[	]0.371, 0.407[	]0.093, 0.272[	0.222	0.037	0.179
6.73	0.506	]0.199, 0.401[	]0.397, 0.401[	]0.099, 0.267[	0.202	0.003	0.168
6.74	0.533	]0.207, 0.397[	(*)	]0.103, 0.265[	0.190	(*)	0.161
6.75	0.598	]0.225, 0.388[	(*)	]0.112, 0.258[	0.163	(*)	0.146

Table 1. Lyapunov exponent, h_{max}, synchronization interval, $\left] \frac{1-e^{-h_{\max}}}{\lambda_2}, \frac{1+e^{-h_{\max}}}{\lambda_N} \right[$, and amplitude of this interval, $\frac{1+e^{-h_{\max}}}{\lambda_N} - \frac{1-e^{-h_{\max}}}{\lambda_2}$, for several intrinsic growth rates r, for the lattices a), b) and c) of Fig.3.(*) In this case, the desynchronization phenomenon occurs, see (C4).

bound. This means that, there is no synchronization for any value of the coupling parameter c. This desynchronization phenomenon was expected because the network (5) synchronizes only if $h_{max} < \ln(2R+1)$, where $R = \frac{\lambda_1 - \lambda_2}{\lambda_2 - \lambda_N}$, see [9]. In the case of lattice b), we have $\ln(2R+1) = 0.511$, so there is synchronization only if $h_{max} < 0.511$, which do not happens for $r = 6.74$ and $r = 6.75$. In all the other studied cases, the Lyapunov exponent verifies $h_{max} < \ln(2R+1)$, so we have a non empty synchronization interval.

Acknowledgment

References

1.A. Balanov, N. Janson, D. Postnov and O. Sosnovtseva. Synchronization: From Simple to Complex, Springer, 2009.
2.G.M. Cailliet, W.D. Smith, H.F. Mollet and K.J. Goldman. Age and growth studies of chondrichthyan fishes: the need for consistency in terminology, verification, validation, and growth function fitting. *Environ. Biol. Fish.*, 77: 211–228, 2006.

3. A.B. Cooper. A Guide to Fisheries Stock Assessment. From Data to Recommendations. New Hampshire Sea Grant, 2006.

4. A.J. Davidson and M. Menaker, Birds of a feather clock together sometimes: social synchronization of circadian rhythms. *Curr. Opin. Neurobiol.*, 13 (6): 765–769, 2003.

5. T.E. Essington, J.F. Kitchell and C.J. Walters. The von Bertalanffy growth function, bioenergetics, and the consumption rates of fish. *Can. J. Fish. Aquat. Sci.*, 58: 2129–2138, 2001.

6. M.Hasler and Y.L. Maistrenko, An introduction to the synchronization of chaotic systems: coupled skew tent maps. *IEEE Trans. on Circ. Syst. – I*, 44 (10): 856–866, 1987.

7. J.A. Hutchings and J.D. Reynolds. Marine fish population collapses: consequences for recovery and extinction isk. *BioSci.*, 54: 297–309, 2004.

8. V.S. Karpouzi and D. Pauly. Life-History Patterns in Marine Birds. In M.L.D. Palomares and D. Pauly, editors, *Fisheries Center Research Reports 16 (10), Von Bertalanffy Growth Parameters of Non-Fish Marine Organisms*, pages 27-43, Canada, 2008. The Fisheries Center, University of British Columbia.

9. X. Li and G. Chen, Synchronization and desynchronization of complex dynamical networks: An engineering viewpoint. *IEEE Trans. on Circ. Syst. –I*, 50 (11): 1381–1390, 2003.

10. D. Lind and B. Marcus. An Introduction to Symbolic Dynamics and Codings. 2nd edition, Cambridge University Press, Cambridge, 1999.

11. J.A. Musick. Criteria to define extinction risk in marine fishes. *Fisheries*, 24: 6–14, 1999.

12. J.L. Rocha and S.M. Aleixo. An extension of gompertzian growth dynamics: Weibull and Fréchet models. *Math. Biosci. Eng.*, 10: 379–398, 2013.

13. J.L. Rocha and S.M. Aleixo. Dynamical analysis in growth models: Blumberg's equation. *Discrete Contin. Dyn. Syst.-Ser.B*, 18: 783–795, 2013.

14. J.L. Rocha, S.M. Aleixo and A. Caneco. Synchronization in Richards' chaotic systems. *Journal of Applied Nonlinear Dynamics*, to appear.

15. S.J. Schreiber. Chaos and population disappearances in simple ecological models. *J. Math. Biol.*, 42: 239–260, 2001.

16. J.A.L. Silva and F.T. Giordani, Density-dependent migration and synchronism in metapopulations. *Bull. of Math. Biol.*, 68: 451465, 2006.

17. L. Von Bertalanffy. A quantitative theory of organic growth. *Human Biology*, 10: 181–213, 1938.

18. L. Von Bertalanffy. Quantitative laws in metabolism and Growth. *The Quarterly Review of Biology*, 32: 217–231, 1957.